more rigorous calculation of the transport properties of model macromolecules.

Acknowledgment. This work was completed while J.G.T. was visiting the Department of Biochemistry of the University of Minnesota, and he thanks Dr. V. A. Bloomfield for his hospitality and for fruitful discussions. S.C.H. is indebted to Dr. H. C. Cheung for his continued guidance and support. This work was supported by grants from the U.S.-Spain Joint Committee for Scientific and Technological Cooperation, from the National Science Foundation (Grant PCM-78-24803), and from the American Cancer Society (Grant IN-66R).

References and Notes

(1) McCammon, J. A.; Deutch, J. M.; Felderhof, B. U. *Biopolymers* **1975**, *14*, 2613.
(2) McCammon, J. A.; Deutch, J. M. *Biopolymers* **1976**, *15*, 1397.
(3) Garcia de la Torre, J.; Bloomfield, V. A. *Biopolymers* **1977**, *16*, 1747.
(4) Garcia de la Torre, J.; Bloomfield, V. A. *Biopolymers* **1977**, *16*, 1765.
(5) Garcia de la Torre, J.; Bloomfield, V. A. *Biopolymers* **1977**, *16*, 1779.
(6) Garcia de la Torre, J.; Bloomfield, V. A. *Biopolymers* **1978**, *17*, 1605.
(7) Wilson, R. W.; Bloomfield, V. A. *Biopolymers* **1979**, *18*, 1205.
(8) Tirado, M. M.; Garcia de la Torre, J. *J. Chem. Phys.* **1979**, *71*, 2581.
(9) Nakajima, H.; Wada, Y. *Biopolymers* **1977**, *16*, 875.
(10) Nakajima, H.; Wada, Y. *Biopolymers* **1978**, *17*, 2291.
(11) Swanson, E.; Teller, D. C.; de Haën, C. *J. Chem. Phys.* **1978**, *68*, 5097.
(12) Yamakawa, Y.; Yoshizaki, T. *Macromolecules* **1979**, *12*, 32.
(13) Hassager, O. *J. Chem. Phys.* **1974**, *60*, 2111.
(14) Wilemski, G. *Macromolecules* **1977**, *10*, 28.
(15) Yamakawa, H. *Macromolecules* **1975**, *8*, 339.
(16) McCammon, J. A.; Wolynes, P. G. *J. Chem. Phys.* **1977**, *66*, 1452.
(17) Ermak, D. L.; McCammon, J. A. *J. Chem. Phys.* **1978**, *69*, 1352.
(18) Harvey, S. C. *J. Chem. Phys.* **1979**, *71*, 4221.
(19) Harvey, S. C. *Biopolymers* **1979**, *18*, 1081.
(20) Harvey, S. C.; Cheung, H. C. *Biopolymers* **1980**, *19*, 913.
(21) Brenner, H. *J. Colloid Interface Sci.* **1967**, *23*, 407.
(22) Happel, J.; Brenner, H. "Low Reynolds Number Hydrodynamics", 2nd ed.; Noordhoff: Leyden, 1973; Chapter 5.
(23) Chandrasekhar, S. *Rev. Mod. Phys.* **1943**, *15*, 1.
(24) Einstein, A. *Ann. Phys.* **1906**, *19*, 371; reprinted in English in: "Investigations on the Theory of Brownian Movement"; Furth, R., Ed.; Dover: New York, 1956; pp 19-35.
(25) Garcia Bernal, J. M.; Garcia de la Torre, J. *Biopolymers* **1980**, *19*, 751.
(26) Symon, K. R. "Mechanics", 2nd ed.; Addison-Wesley: Reading, MA, 1960; Chapter 5.

Theory of Unsymmetric Polymer–Polymer Interfaces in the Presence of Solvent

K. M. Hong and J. Noolandi*

Xerox Research Center of Canada, Mississauga, Ontario, Canada, L5L 1J9.
Received December 21, 1979

ABSTRACT: A theory is presented of the interfacial properties between two immiscible polymers in the presence of a solvent. We use diffusion equations for the probability densities characterizing the polymer configurations, derived on the basis of the mean-field approximation for the intermolecular interactions. We consider systems with a small compressibility and, for specific calculations, we assume the Flory–Huggins form for the free energy. In the limit of infinite molecular weight for the polymers we solve the mean-field equations numerically to obtain the interfacial tension and density profiles for typical values of the interaction parameters. Calculations for the system poly(dimethylsiloxane)–benzene–polystyrene are also carried out.

In recent years there has been considerable interest in the theory of the interfacial properties of heterogeneous polymeric systems. This interest has been motivated to a great extent by the increasingly important role that polymer blends, grafts, and blocks are playing in modern technology. The use of block copolymers in the development of thermoplastic elastomers, hot melt extrudable adhesives, and protective coatings are but some of the important commercial applications currently in use.[1]

Recently Helfand[2-5] has focused on the details of the microdomain structure of block copolymers and has developed a theory, based on mean-field ideas, for predicting domain sizes for various geometries. However, relatively little work has been done to extend the theory of inhomogeneous polymers to include the effects of solvents, which can have a marked influence on the phase separation and physical properties of block copolymer systems.[6] In this paper we present a theory for predicting interfacial properties between two immiscible homopolymers in the presence of a solvent. Our theoretical formulation constitutes an extension of some recent work by Helfand and Sapse[7] on the saturated homopolymer–solvent interface.

In section I we present the theory, based on the mean-field approximation, and discuss the effect of including nonlocal interactions in the free energy. Although our formulation is quite general, we make use of the Flory–Huggins form of the free energy for specific calculations. Section II contains the calculation of the asymptotic (bulk) properties of the polymer–solvent phases away from the interface and leads to a discussion of the equilibrium phase diagrams for the ternary system. Our free energy density contains a term to suppress local fluctuations in the density which would otherwise accompany phase separation, contrary to observation. The determination of this term, in the limit of zero compressibility, is given in section IIB. The numerical method used to solve the mean-field equations is given in section III, along with calculations of the interfacial density profiles and interfacial tensions for typical interaction parameters. Results for the system PDMS/benzene/PS are given in section IV.

I. Formulation of Theory

A. Mean-Field Approximation. We begin by introducing some standard nomenclature for the quantities of

0024-9297/80/2213-0964$01.00/0

interest in this problem.[7] The densities of pure material, in monomer segments per unit volume, will be denoted by ρ_{0K}, where K refers to the polymer (subscripts A or B) or to the solvent (subscript S). The corresponding reduced densities are defined by

$$\tilde{\rho}_K = \rho_K/\rho_{0K} \tag{1}$$

The asymptotic reduced densities in the homogeneous polymer–solvent mixtures away from the interface will be denoted by $\tilde{\rho}_A(-\infty)$ and $\tilde{\rho}(\infty)$ with the convention that the polymer A–solvent mixture is to the left of the interface. The degree of polymerization of a part of a larger molecule is denoted by t, and t can vary between 0 and Z_K, the degree of polymerization of the whole molecule. The Kuhn statistical length of a single segment of K is b_K.

The mean-field equations determine a quantity $q_K(\mathbf{r}, t)$ which is proportional to the probability density that the end of a molecule of type K and degree of polymerization t is at $\mathbf{r}$ and take the form[2]

$$\frac{\partial q_K}{\partial t} = \left(\frac{b_K^2}{6}\nabla^2 - \frac{1}{k_BT}\frac{\partial \Delta f}{\partial \rho_K}\right) q_K \tag{2}$$

with the initial condition

$$q_K(\mathbf{r}, 0) = 1 \tag{3}$$

and the boundary conditions that $q_K(\mathbf{r}, t)$ approach a constant in the bulk K phase and its gradient vanish in the other phase. The second term in parentheses in eq 2 represents the "effective" or mean field, and the quantity Δf is the free energy density of a mixture of densities ρ_A, ρ_B, and ρ_S less the free energy density in the bulk away from the interface. The form of Δf will be discussed later.

In order to solve the set of equations (2), we must use the relation between $q_K(\mathbf{r}, t)$ and the density $\rho_K(\mathbf{r})$:[2]

$$\rho_K(\mathbf{r}) = \frac{N_K}{Z_K}\int_0^{Z_K} dt\; q_K(\mathbf{r}, Z_K - t)q_K(\mathbf{r}, t)/\int d^3r\; q_K(\mathbf{r}, Z_K) \tag{4}$$

In eq 4 N_K is the number of K monomer units. For $Z_K \to \infty$, as we assume in this paper, eq 4 reduces to simply

$$\rho_A(\mathbf{r}) = \rho_A(-\infty)q_A^2(\mathbf{r})$$
$$\rho_B(\mathbf{r}) = \rho_B(\infty)q_B^2(\mathbf{r}) \tag{5}$$

and we need only to find the "steady-state" solutions of eq 2, which reduce to

$$\frac{b_A^2}{6}q_A'' = \frac{1}{k_BT}\frac{\partial \Delta f}{\partial \rho_A}q_A$$
$$\frac{b_B^2}{6}q_B'' = \frac{1}{k_BT}\frac{\partial \Delta f}{\partial \rho_B}q_B \tag{6}$$

where we have made use of the one-dimensional nature of the single interface problem. In addition to eq 6, the constancy of the chemical potential of the solvent requires

$$0 = \partial \Delta f/\partial \rho_S \tag{7}$$

The solution of eq 6 and 7 for the Flory–Huggins form of the free energy density is discussed in section III. An important quantity which characterizes the interface is the interfacial tension, given in the mean-field approximation by[2]

$$\gamma = 2\int_{-\infty}^{+\infty} dx\; \Delta f \tag{8}$$

Calculations of the concentration profiles of the polymers as well as the interfacial tension are given in sections III and IV for varying amounts of solvent in the ternary system.

B. Flory–Huggins Free Energy Density. The Flory–Huggins (FH) form of the free energy density is[8]

$$\Delta f = \rho_A(\mu_{0A} - \mu_A) + \rho_B(\mu_{0B} - \mu_B) + \rho_S(\mu_{0S} - \mu_S) + k_BT\left\{\frac{\alpha_{AB}\tilde{\rho}_A\tilde{\rho}_B + \alpha_{AS}\tilde{\rho}_A\tilde{\rho}_S + \alpha_{BS}\tilde{\rho}_B\tilde{\rho}_S}{\tilde{\rho}_A + \tilde{\rho}_B + \tilde{\rho}_S} + \rho_{0S}\tilde{\rho}_S \ln\left(\frac{\tilde{\rho}_S}{\tilde{\rho}_A + \tilde{\rho}_B + \tilde{\rho}_S}\right) + \frac{1}{2\kappa k_BT}(\tilde{\rho}_A + \tilde{\rho}_B + \tilde{\rho}_S - 1)^2\right\} \tag{9}$$

where we have assumed infinite molecular weight for the polymers; hence we need not discuss the so-called "kinetic" terms, which depend inversely on the degree of polymerization. The free energy density is written with respect to its value in the asymptotic phases, with the convention that polymer A is to the left of the interface, as specified earlier. The differences of the chemical potentials from the values in the pure materials will be determined from the theoretical calculations.

The first term inside the braces in eq 9 corresponds to the usual FH energy of uniform mixing of the three components, written in terms of mixing parameters $\alpha_{KK'}$, which will later be related to the $\chi_{KK'}$ parameters. The second term in the braces gives the entropy of mixing of the solvent small molecules, and the last term restricts the size of density fluctuations in the system. Since the compressibility κ is usually very small, the partial derivative of this term becomes indeterminate in the limit of negligible volume change upon mixing, and it must be obtained self-consistently from the theory, as described in section IIB. As discussed in the literature, effects such as a composition dependence of κ and small volume changes of mixing can also be included in the theory.[3] However, we will neglect these refinements in our calculations.

C. Nonlocal Effects.

A minor modification which is relatively easy to include in the theory is the addition of nonlocal effects. Briefly, nonlocal terms arise from the finite range of a general interaction potential between different molecules, assumed to be of the form

$$\int d^3r\; d^3r'\; \tilde{\rho}_K(\mathbf{r})\tilde{\alpha}_{KK'}(\mathbf{r} - \mathbf{r}')\rho_{K'}(\mathbf{r}') \tag{10}$$

Assuming that the potential is slowly varying, a gradient expansion of eq 10 gives for the corresponding effective field[7]

$$\frac{1}{k_BT}\frac{\partial \Delta f}{\partial \rho_K} = \frac{1}{\rho_{0K}}\int d^3r'\; \tilde{\alpha}_{KK'}(\mathbf{r} - \mathbf{r}')\tilde{\rho}_{K'}(\mathbf{r}') \simeq \frac{\alpha_{KK'}}{\rho_{0K}}\tilde{\rho}_{K'}(\mathbf{r}) + \frac{\sigma_{KK'}^2\alpha_{KK'}}{6\rho_{0K}}\nabla^2\tilde{\rho}_{K'}(\mathbf{r}) + \ldots \tag{11}$$

where

$$\alpha_{KK'} = \int d^3s\; \tilde{\alpha}_{KK'}(\mathbf{s})$$
$$\sigma_{KK'}^2 = \int d^3s\; s^2\tilde{\alpha}_{KK'}(\mathbf{s})/\int d^3s\; \tilde{\alpha}_{KK'}(\mathbf{s}) \tag{12}$$

and the nonlocal contribution to the free energy is of the form

$$\Delta f_{\text{nonlocal}} = \frac{k_BT}{12}\sum_{KK'}\alpha_{KK'}\sigma_{KK'}^2\int d^3r\; \nabla\tilde{\rho}_K(\mathbf{r})\cdot\nabla\tilde{\rho}_{K'}(\mathbf{r}) \tag{13}$$

In practice, the quantity $\sigma_{KK'}$ is taken to be of the order of the average of b_K and $b_{K'}$ for the macromolecules.

Including the nonlocal terms, eq 6 and 7 become

$$\frac{b_A^2}{6}q_A'' = \frac{1}{k_BT}\frac{\partial \Delta f}{\partial \rho_A}q_A + \frac{1}{6\rho_{0A}}(\alpha_{AB}\sigma_{AB}^2\tilde{\rho}_B'' + \alpha_{AS}\sigma_{AS}^2\tilde{\rho}_S'')q_A$$

$$\frac{b_B^2}{6}q_B'' = \frac{1}{k_BT}\frac{\partial \Delta f}{\partial \rho_B}q_B + \frac{1}{6\rho_{0B}}(\alpha_{AB}\sigma_{AS}^2\tilde{\rho}_A'' + \alpha_{BS}\sigma_{BS}^2\tilde{\rho}_S'')q_B \quad (14)$$

and

$$0 = \frac{1}{k_BT}\frac{\partial \Delta f}{\partial \rho_S} + \frac{1}{6\rho_{0S}}(\alpha_{AS}\sigma_{AS}^2\tilde{\rho}_A'' + \alpha_{BS}\sigma_{BS}^2\tilde{\rho}_B'') \quad (15)$$

II. Asymptotic Phases

A. Phase Diagrams. From the FH free energy density, eq 9, we obtain the expressions for the effective fields

$$\frac{\partial \Delta f}{\partial \rho_A} = \mu_{0A} - \mu_A + \frac{k_BT}{\rho_{0A}}\{\alpha_{AB}\phi_B^2 + \alpha_{AS}\phi_S^2 + (\alpha_{AB} + \alpha_{AS} - \alpha_{BS})\phi_B\phi_S - \rho_{0S}\phi_S + \omega\} \quad (16)$$

where we have defined the volume fractions

$$\phi_A = \frac{\tilde{\rho}_A}{(\tilde{\rho}_A + \tilde{\rho}_B + \tilde{\rho}_S)} \quad (17)$$

etc., and

$$\omega = \frac{1}{\kappa k_BT}(\tilde{\rho}_A + \tilde{\rho}_B + \tilde{\rho}_S - 1) \quad (18)$$

In the limit $\kappa \to 0$, we have $\sum\tilde{\rho}_K = 1$, since there is no volume change upon mixing, and the expression for ω, eq 18, becomes indeterminate. The calculation of ω in this case is given in section IIB. The expression for $\partial\Delta f/\partial\rho_B$ is similar to eq 16, and

$$\frac{\partial \Delta f}{\partial \rho_S} = \mu_{0S} - \mu_S + \frac{k_BT}{\rho_{0S}}\{\alpha_{AS}\phi_A^2 + \alpha_{BS}\phi_B^2 + (\alpha_{AS} + \alpha_{BS} - \alpha_{AB})\phi_A\phi_B + \rho_{0S}\ln\phi_S + \rho_{0S}(1 - \phi_S) + \omega\} \quad (19)$$

In the asymptotic phases the effective fields as well as the function $\omega(x)$ vanish, and noting that the chemical potential is constant we obtain from eq 19

$$\mu_S - \mu_{0S} = \frac{k_BT}{\rho_{0S}}\{\alpha_{AS}\phi_A^2(-\infty) + \rho_{0S}\ln\phi_S(-\infty) + \rho_{0S}[1 - \phi_S(-\infty)]\}$$
$$= \frac{k_BT}{\rho_{0S}}\{\alpha_{BS}\phi_B^2(\infty) + \rho_{0S}\ln\phi_S(\infty) + \rho_{0S}[1 - \phi_S(\infty)]\} \quad (20)$$

giving the following relation between the volume fractions of polymer in the two asymptotic phases

$$\chi_{AS}\phi_A^2(-\infty) + \phi_A(-\infty) + \ln[1 - \phi_A(-\infty)] = \chi_{BS}\phi_B^2(\infty) + \phi_B(\phi) + \ln[1 - \phi_B(\infty)] \quad (21)$$

where we have defined

$$\chi_{AS} = \alpha_{AS}/\rho_{0S};\ \chi_{BS} = \alpha_{BS}/\rho_{0S} \quad (22)$$

Equation 21, along with the relation

$$\frac{\phi_A^0}{\phi_A(-\infty)} + \frac{\phi_B^0}{\phi_B(\infty)} = 1 \quad (23)$$

which follows from the division of the mixed system into an A-solvent volume fraction and a B-solvent volume fraction, where ϕ_A^0 and ϕ_B^0 are the unmixed volume fractions of A and B, allows for the construction of the standard phase diagrams shown in Figures 1 and 2. For any choice of unmixed volume fractions, we can calculate by eq 21 and 23 the tie lines and the composition of the mixed homogeneous phases. The tie line bounding the three-phase region is obtained from eq 20 by setting $\mu_S = \mu_{0S}$.

The shift of the chemical potentials for polymers A and B in the asymptotic phases can be derived in the same way

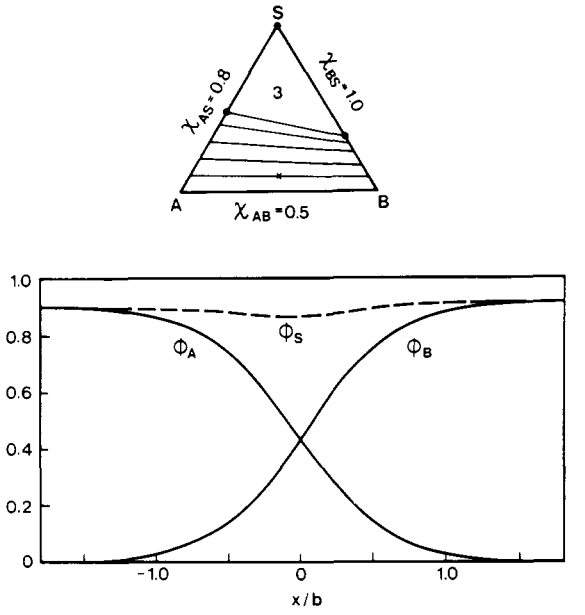

Figure 1. Interfacial concentration profiles of polymers (A, B) and solvent (S) corresponding to point × on the phase diagram shown above. The values of the χ parameters are indicated on the phase diagram, and the three-phase region is shown by the inner triangle. The distance from the interface is measured in units of the Kuhn length b, which is taken to be the same for the two polymers in this model calculation. The solvent volume fraction is measured from the top down.

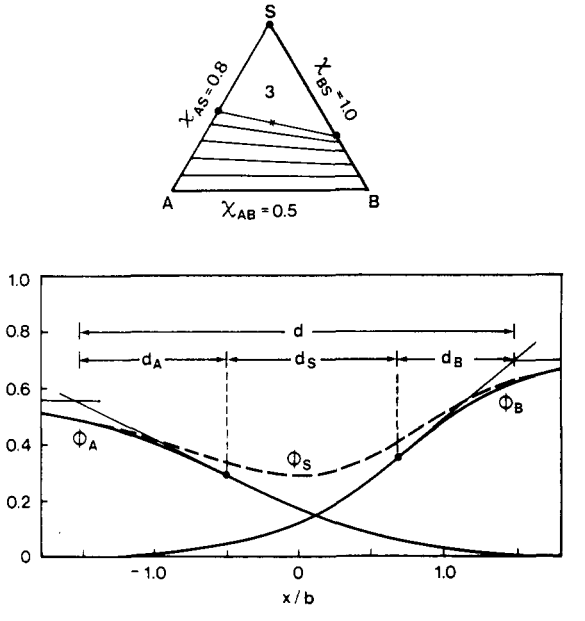

Figure 2. Interfacial concentration profiles of polymers (A, B) and solvent (S) corresponding to point × on the phase diagram shown above. The χ values are the same as in Figure 1, and the three-phase region is shown by the inner triangle. The inflection points of the polymer concentration profiles are used to define a solvent-rich region (width d_S), and the polymer-A- and -B-rich regions (widths d_A and d_B) are bounded by the intersections of the tangents at the inflection points with the lines corresponding to the asymptotic polymer concentrations. The solvent volume fraction is measured from the top down.

as eq 20; eliminating these quantities from the equations for the effective fields of the polymers gives

$$\frac{1}{k_BT}\frac{\partial \Delta f}{\partial \rho_A} = \frac{1}{\rho_{0A}}\{\alpha_{AB}\phi_B^2 + \alpha_{AS}[\phi_S^2 - \phi_S^2(-\infty)] + (\alpha_{AB} + \alpha_{AS} - \alpha_{BS})\phi_B\phi_S + \rho_{0S}[\phi_S(-\infty) - \phi_S] + \omega\}$$

$$\frac{1}{k_BT}\frac{\partial \Delta f}{\partial \rho_B} = \frac{1}{\rho_{0B}}\{\alpha_{AB}\phi_A^2 + \alpha_{BS}[\phi_S^2 - \phi_S^2(\infty)] + (\alpha_{AB} + \alpha_{BS} - \alpha_{AS})\phi_A\phi_S + \rho_{0S}[\phi_S(\infty) - \phi_S] + \omega\} \quad (24)$$

Finally we need an expression for the indeterminate function ω before we can use the above results for the effective fields and proceed with the solution of eq 14.

B. Elimination of Indeterminate Form. Using eq 15, 19, and 20, we find the following expressions for ω:

$$\omega = -\tfrac{1}{6}(\alpha_{AS}\sigma_{AS}^2\phi_A'' + \alpha_{BS}\sigma_{BS}^2\phi_B'') + \{\alpha_{AS}[\phi_A^2(-\infty) - \phi_A^2] - [\alpha_{BS}\phi_B^2 + (\alpha_{AS} + \alpha_{BS} - \alpha_{AB})\phi_A\phi_B] + \rho_{0S}\ln[\phi_S(-\infty)/\phi_S] + \rho_{0S}[\phi_S - \phi_S(-\infty)]\} \quad (25)$$

or

$$\omega = -\tfrac{1}{6}(\alpha_{AS}\sigma_{AS}^2\phi_A'' + \alpha_{BS}\sigma_{BS}^2\phi_B'') + \{\alpha_{BS}[\phi_B^2(\infty) - \phi_B^2] - [\alpha_{AS}\phi_A^2 + (\alpha_{AS} + \alpha_{BS} - \alpha_{AB})\phi_A\phi_B] + \rho_{0S}\ln[\phi_S(\infty)/\phi_S] + \rho_{0S}[\phi_S - \phi_S(\infty)]\} \quad (26)$$

Using either of these expressions and eq 14 and 24, as well as the relations $q_A^2 = \phi_A/\phi_A(-\infty)$ and $q_A^2 = \phi_B/\phi_B(\infty)$, we can proceed to solve for the concentration profiles of the three components in the interfacial region.

III. Interfacial Properties

A. Numerical Method. For the numerical solution of eq 14 we introduced $b = (b_A + b_B)/2$ as the unit of length and divided the interfacial region into discrete sections such that $x/b = n\delta$, where δ is a constant. In our calculations we took n to be in the range −50 to +50, and we chose $\delta \sim 0.4$ typically for a broad interface corresponding to a small χ_{AB} or a high solvent concentration (Figure 1) and $\delta \sim 0.2$ for a narrow interface (Figure 2). For the calculation of the concentration profiles the asymptotic values of q were fixed; e.g., $q_B(-50) = 0$, $q_B(50) = 1$, with $\rho_B(n) = \rho_B(\infty)q_B^2(n)$. The asymptotic volume fractions of polymers A and B and hence the asymptotic densities were determined as outlined in section IIA. The initial trial function for the numerical solution was chosen to be

$$q_B(n) = \{\tfrac{1}{2}[1 + \tanh\{(6\chi_{AB})^{1/2}x/b\}]\}^{1/2} \quad (27)$$

for n in the range −49 to +49, with a similar expression for $q_A(n)$. Equation 27 represents the analytic solution for the interfacial profile of an immiscible (symmetric) homopolymer system,[9] without solvent, and serves as a good starting approximation for numerical calculations on the ternary system.

Equations 14, which are of the form

$$q_B'' = F(q_A, q_B) \quad (28)$$

were solved by the generalized Newton method.[10] In this numerical scheme the differences

$$\Delta q_B(n) = \frac{\lambda\delta^2}{2}\left\{\frac{[q_B(n+1) - 2q_B(n) + q_B(n-1)]/\delta^2 - F(q_A, q_B)}{1 + \frac{\delta^2}{2}\frac{\partial F}{\partial q_B(n)}}\right\} \quad (29)$$

were calculated, starting with $n = 49$, say, and using the new value of $q_B(n=49)$ defined by

$$(\text{new})q_B(n=49) = (\text{old})q_B(n=49) + \Delta q_B(n=49) \quad (30)$$

in the equation for $\Delta q_B(n=48)$, and so on. This operation was continued until the interfacial region was traversed and then repeated in its entirety until convergence was obtained. The overrelaxation factor λ was chosen to improve the covergence of this procedure. For broad interfaces, $\lambda \sim 1.5$, while for narrow interfaces, $\lambda \sim 1$. The results of these calculations are discussed in the remainder of this section.

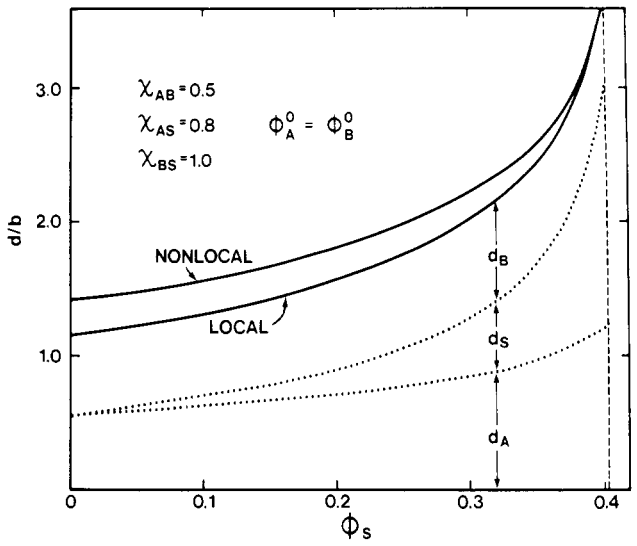

Figure 3. Total width of interface (solid line) and components (dotted lines) in reduced units as a function of the volume fraction of solvent, for the phase diagrams shown in Figures 1 and 2. The volume fractions of the two polymers are assumed to be equal, corresponding to a trajectory on the phase diagram along the perpendicular from the vertex S to the line AB. The dashed line indicates the volume fraction at which the polymers become saturated with solvent and a three-phase region appears. Also shown is the calculated total width taking into account nonlocal interactions.

B. Concentration Profiles. Figure 1 shows the calculated interfacial concentration profiles of the different components of the ternary system, corresponding to the point indicated on the phase diagram. For this model calculation we have assumed $b_A = b_B = b$ and $\rho_{0A} = \rho_{0B} = \rho_{0S} = \rho_0$. The polymer–polymer interaction parameter is defined by

$$\chi_{AB} = \alpha_{AB}/\rho_{0S} \quad (31)$$

For the case of small ϕ_S^0 shown in Figure 1, there is very little accumulation of the solvent in the interfacial region. This diagram should be compared to Figure 2, where we show the interfacial profiles for a point on the phase diagram bordering the three-phase region. In this case we see that the presence of the solvent results in considerable broadening of the interface.

In Figure 2 we have singled out the inflection points of the polymer profiles in order to define solvent- and polymer-rich regions. Figure 3 shows the variation of the interfacial thickness, divided into three components, for increasing amounts of solvent in the system. It is interesting to note that the widths of the polymer-rich regions remain approximately the same, while the width of the solvent-rich region increases with increasing solvent concentration. The dashed line indicates the point at which the polymers become saturated with solvent and the system separates into three phases. The interfacial profiles shown in Figures 1 and 2 were calculated by using the model with only local interaction parameters. The effect of the nonlocal interactions, calculated with $\sigma \sim b$ (section IC), is to increase the total width of the interface slightly, leaving the details of the profiles almost unaffected. Figure 4 shows the variation of the interfacial tension with in-

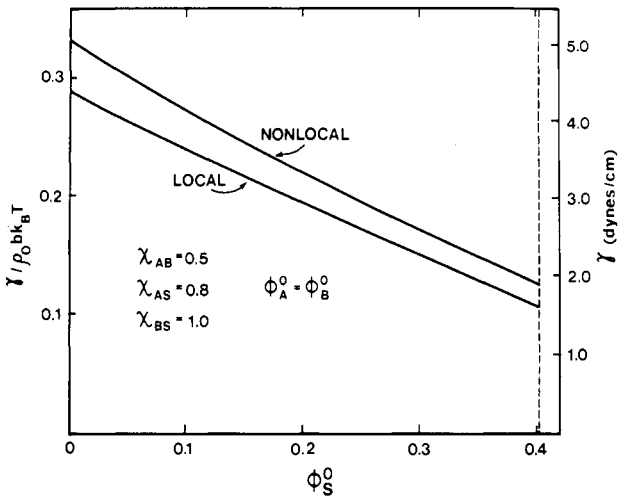

Figure 4. Interfacial tension γ as a function of solvent volume fraction for the same conditions as in Figure 3. The left-hand scale is in reduced units; for the right-hand scale, $\rho_0 bk_BT \sim 15$ dyn/cm, using b = 6 Å, $\rho_{0A} = \rho_{0B} = \rho_{0S}$ = 0.01 mol/cm^3, and T = 298 K.

creasing solvent concentration. The effect of the nonlocal interactions in this case is to increase the calculated values by 15–20%.

IV. Calculations for PDMS/Benzene/PS

The calculations for this interface were carried out for T = 25 °C, using ρ_{PS} = 1.0711 g cm^{-3},[11] ρ_{PDMS} = 0.9699 g cm^{-3},[12] $\rho_{benzene}$ = 0.8738 g cm^{-3},[13] b_{PS} = 6.6 Å, and b_{PDMS} = 5.8 Å.[3] In the absence of more complete experimental information, we used $\chi_{PS\text{-}benzene}$ = 0.455,[14] obtained in the infinite-dilution limit, for the whole range of benzene concentration. A range of values has been measured for $\chi_{PDMS\text{-}benzene}$, from 0.82 to 0.48, depending on the volume fraction of benzene.[15] $\chi_{PS\text{-}PDMS}$ was calculated from the expression involving the Hildebrand solubility parameters[16]

$$\chi_{AB} = (V_r/k_BT)(\delta_A - \delta_B)^2 \qquad (32)$$

using δ_{PS} = 9.0 cal$^{1/2}$ cm$^{2/3}$,[17] and δ_{PDMS} = 7.5 cal$^{1/2}$ cm$^{2/3}$ [18] and taking the reference volume V_r (in cm^3/mol) to be that of benzene at T = 25 °C, giving $\chi_{PS\text{-}PDMS}$ = 0.34.

The calculated width of the interface as a function of benzene concentration is shown in Figure 5. With the quoted values of the χ parameters, this system does not have a three-phase region. The effect of the nonlocal terms in the free energy on the total width is found to be very small. Figure 6 shows the calculated interfacial tension corresponding to Figure 5. There are a number of problems in comparing this curve to experiment. First, the reliability of some of the χ parameters we have used could be improved. Second, the temperature for which we have carried out our calculations, T = 25 °C, is below the glass transition temperature for polystyrene, $T_g^{PS} \sim$ 100 °C,[19] so that for small concentrations of benzene the system solidifies and the present theory is no longer valid. The problem with carrying out calculations at higher temperatures, where the polymers are molten, is that the χ parameters are even more poorly known. Measurements at T = 100 °C give $\gamma_{PS\text{-}PDMS}$ = 6.1 dyn/cm,[20] in the absence of benzene, with a very small temperature coefficient from T = 100 to T = 180 °C. In spite of the limitations of the extrapolation procedure, our values for $\phi^0_{benzene}$ = 0 at T = 25 °C give γ_{local} = 4.13 dyn/cm and $\gamma_{nonlocal}$ = 4.55 dyn/cm, close to the measured value at T = 100 °C.

Although the point has been made earlier, it is worth repeating that progress in the theory of interfaces of polymeric systems can only be made on the basis of careful

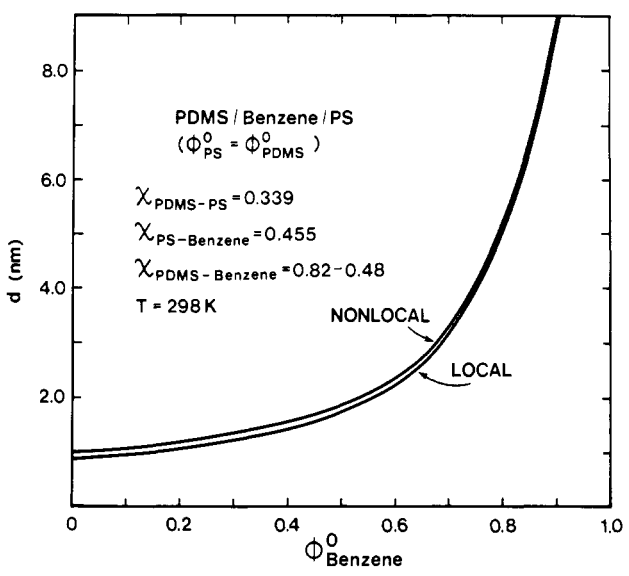

Figure 5. Total width of interface for the system PDMS/benzene/PS as a function of benzene volume fraction, showing results for both local and nonlocal theories. A range of χ values for PDMS/benzene was used, depending on the benzene volume fraction.

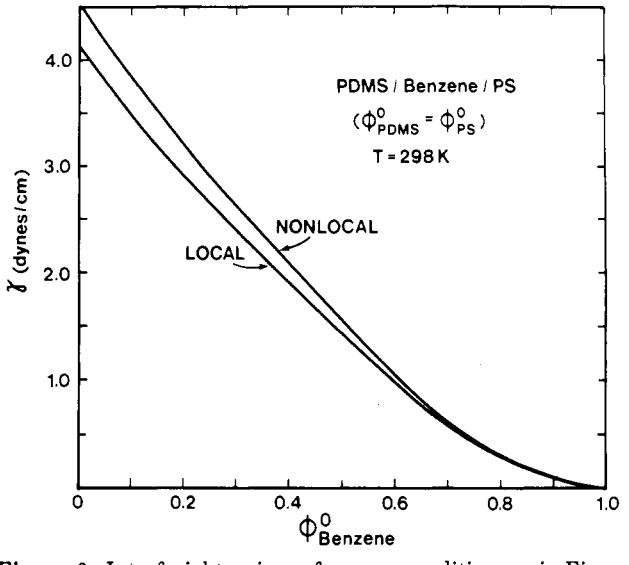

Figure 6. Interfacial tension γ for same conditions as in Figure 5.

measurements of the fundamental interaction parameters, carried out over a wide range of temperature and composition.

Acknowledgment. We thank L. M. Marks for developing the computer program used to evaluate the interfacial density profiles and for assistance with the numerical calculations.

References and Notes

(1) L. H. Sperling, Ed., *Polym. Sci. Technol.*, 4 (1974).
(2) E. Helfand, *J. Chem. Phys.*, 62, 999 (1975).
(3) E. Helfand and A. M. Sapse, *J. Chem. Phys.*, 62, 1327 (1975).
(4) E. Helfand and Z. R. Wasserman, *Macromolecules*, 9, 879 (1976).
(5) E. Helfand and Z. R. Wasserman, *Macromolecules*, 11, 960 (1978).
(6) S. L. Aggarwal, Ed., Block Copolymers, Plenum Press, New York, 1970.
(7) E. Helfand and A. M. Sapse, *J. Polym. Sci., Polym. Symp.*, No. 54, 289 (1976).
(8) P. J. Flory, "Principles of Polymer Chemistry", Cornell University Press, Ithaca, NY, 1953.
(9) E. Helfand and Y. Tagami, *J. Chem. Phys.*, 56, 3592 (1972).

(10) D. Greenspan, "Discrete Numerical Methods in Physics and Engineering", Academic Press, New York, 1974, Chapter I.
(11) H. Höcker, G. J. Blake, and P. J. Flory, *Trans. Faraday Soc.*, **67**, 2251 (1971).
(12) H. Shih and P. J. Flory, *Macromolecules*, **5**, 758 (1972).
(13) S. E. Wood and J. P. Brusic, *J. Am. Chem. Soc.*, **65**, 1891 (1943).
(14) R. A. Orwoll, *Rubber Chem. Technol.*, **50**, 451 (1977).
(15) P. J. Flory and H. Shih, *Macromolecules*, **5**, 761 (1972).
(16) S. Krause, *Polym. Blends. 1978*, 1 (1978).
(17) P. J. Hoftyzer and D. W. VanKrevelen, *Int. Symp. Macromol. IUPAC, Leyden* (1970); D. W. Van Krevelen, "Properties of Polymers", Elsevier, Amsterdam, 1972, Chapters 6 and 8.
(18) J. Brandrup and E. H. Immergut, "Polymer Handbook", Interscience, New York, 1966.
(19) *Encycl. Polym. Sci. Technol.*, **13**, 244 (1970).
(20) S. Wu., *J. Macromol. Sci., Rev. Macromol. Chem.*, **C10** (1), 1 (1974).

Characterization of Polymer Compatibility by Nonradiative Energy Transfer. Application to Binary Mixtures Containing Anionically Prepared Polystyrene, Anionically Prepared Poly(α-methylstyrene), or Poly(2,6-dimethyl-1,4-phenylene ether)

F. Mikeš[1] and H. Morawetz*

Polymer Research Institute, Polytechnic Institute of New York, Brooklyn, New York 11201

K. S. Dennis

Dow Chemical Co., Midland, Michigan 48640. *Received January 22, 1980*

ABSTRACT: Polystyrene (PS) and poly(α-methylstyrene) (PMS), prepared by anionic polymerization, and poly(2,6-dimethyl-1,4-phenylene ether) (PPO) were labeled with carbazole or anthracene residues. The compatibility of polymer pairs labeled with the donor and acceptor chromophores, respectively, was characterized by nonradiative energy transfer in blends of PS with PMS, PPO with PS, and PPO with PMS. The technique demonstrates a slight departure from random mixing even in the PPO–PS system, which has been previously described as perfectly compatible.

In a previous report from this laboratory[2] a new method was demonstrated by which the compatibility of two polymers can be characterized. In this technique the first polymer was labeled with a fluorescent residue (the "donor") whose emission spectrum overlapped the absorption spectrum of another fluorescent moiety (the "acceptor") attached to the second polymeric species. Energy absorbed by the donor can then be transferred by a nonradiative process to the acceptor over distances of the order of 2 nm so that the relative donor and acceptor emission intensities of a sample irradiated in the donor absorption band is a measure of the spacing of donor and acceptor groups and thus dependent on the mutual interpenetration of the two polymeric species.

In this previous work the fluorescent labels were introduced into the polymers by copolymerization. In the present study we have developed techniques by which such labels may be attached to preexisting aromatic polymers. This allowed us to use polystyrene and poly(α-methylstyrene) with narrow molecular weight distributions prepared by the "living polymer" polymerization technique. It allowed us also to investigate the compatibility characteristics of poly(2,6-dimethyl-1,4-phenylene ether), which had been studied previously by a variety of methods.[4-8]

Experimental Section

Polymers. Polystyrene (PS) and poly(α-methylstyrene) (PMS) were prepared by anionic polymerization, using potassium naphthalene as the initiator. The molecular-weight distribution was characterized by GPC, yielding for PS $\bar{M}_n = 11.3 \times 10^4$ and $\bar{M}_w = 17.1 \times 10^4$ and for PMS $\bar{M}_n = 9.49 \times 10^4$ and $\bar{M}_w = 11.9 \times 10^4$. The polymers were twice dissolved and reprecipitated to remove residual naphthalene. Poly(2,6-dimethyl-1,4-phenylene ether) (PPO) was a gift from Dr. D. Fox of the General Electric Co. It had $[\eta] = 0.49$ dL/g in chloroform at 25 °C.

Attachment of Fluorescent Labels. PS and PMS were chloromethylated as described by Jones.[9] With 1 wt % of $ZnCl_2$ added to a 10% polymer solution in chloromethyl methyl ether, chlorine contents of 0.85 wt % in PS and 0.53 wt % in PMS were obtained after 10 min at room temperature. To ensure complete removal of the $ZnCl_2$, the modified polymers were dissolved in dioxane and reprecipitated in water.

The chloromethylated PS and PMS were condensed with potassium carbazole as described by Gibson and Bailey.[10] The polymer was dissolved and reprecipitated five times with intermittent washing by the precipitant until the absorption in the 270–320-nm range, characteristic of carbazole, stopped decreasing.

Anthracene-labeled PS and PMS were prepared by treating the chloromethylated polymers with (9-anthryl)methanol (Aldrich) and sodium hydride by the procedure used for the benzylation of carbohydrates.[11] This method is based on the observation[12] that benzyl chloride does not react with sodium hydride below 170 °C.

The fluorescent labels were attached to poly(2,6-dimethyl-1,4-phenylene ether) (PPO) by first slightly chlorinating the polymer in refluxing chloroform and then reacting the chloromethyl groups with potassium carbazole or (9-anthryl)methanol as described above.

The content of carbazole and anthracene moieties in the polymers was determined by UV spectroscopy, using dioxane solutions for labeled PS and PMS and chloroform solutions for labeled PPO. The extinction coefficients were assumed to be the same as those of 9-benzylcarbazole (ϵ 16 070 and ϵ 16 210 cm^{-1} M^{-1} at 294 nm in dioxane and chloroform, respectively) and (9-anthryl)methanol (ϵ 8460 and ϵ 8530 cm^{-1} M^{-1} at 365 nm in dioxane and chloroform, respectively). The absorption spectra of the labeled polymers in the region characteristic of the carbazole and anthracene moieties were identical with those of the low molecular weight derivatives.

Sample Preparation and Fluorescence Measurements. Films were cast from tetrahydrofuran solutions containing PS–PMS blends and from methylene chloride solutions containing PPO–PS or PPO–PMS blends. In all cases the labeled polymers

0024-9297/80/2213-0969$01.00/0